

## Article

# Spatial patterns in temperature sensitivity of soil respiration in China: Estimation with inverse modeling

ZHOU Tao<sup>1,2†</sup>, SHI PeiJun<sup>1,2</sup>, HUI DaFeng<sup>3</sup> & LUO YiQi<sup>4</sup><sup>1</sup> State Key Laboratory of Earth Surface Processes and Resource Ecology, Beijing Normal University, Beijing 100875, China;<sup>2</sup> Academy of Disaster Reduction and Emergency Management, Ministry of Civil Affairs & Ministry of Education, Beijing 100875, China;<sup>3</sup> Department of Biological Sciences, Tennessee State University, Nashville, TN 37209, USA;<sup>4</sup> Department of Botany and Microbiology, University of Oklahoma, Norman, OK 73019, USA

Temperature sensitivity of soil respiration ( $Q_{10}$ ) is an important parameter in modeling the effects of global warming on ecosystem carbon release. Experimental studies of soil respiration have ubiquitously indicated that  $Q_{10}$  has high spatial heterogeneity. However, most biogeochemical models still use a constant  $Q_{10}$  in projecting future climate change and no spatial pattern of  $Q_{10}$  values at large scales has been derived. In this study, we conducted an inverse modeling analysis to retrieve the spatial pattern of  $Q_{10}$  in China at 8 km spatial resolution by assimilating data of soil organic carbon into a process-based terrestrial carbon model (CASA model). The results indicate that the optimized  $Q_{10}$  values are spatially heterogeneous and consistent to the values derived from soil respiration observations. The mean  $Q_{10}$  values of different soil types range from 1.09 to 2.38, with the highest value in volcanic soil, and the lowest value in cold brown calcic soil. The spatial pattern of  $Q_{10}$  is related to environmental factors, especially precipitation and top soil organic carbon content. This study demonstrates that inverse modeling is a useful tool in deriving the spatial pattern of  $Q_{10}$  at large scales, with which being incorporated into biogeochemical models, uncertainty in the projection of future carbon dynamics could be potentially reduced.

temperature sensitivity,  $Q_{10}$ , soil respiration, global warming, inverse analysis

Soil respiration in terrestrial ecosystems plays a critical role in regulating global carbon cycling. One significant factor that not only influences the response of soil respiration to global change but also determines the direction and magnitude of terrestrial carbon cycle feedback to climate warming is temperature sensitivity of soil respiration<sup>[1,2]</sup>. Temperature sensitivity (often termed as  $Q_{10}$ ) is a factor by which soil respiration is multiplied when temperature increases by 10°C<sup>[3]</sup>.  $Q_{10}$  is often used as an important parameter in biogeochemical models to predict ecosystem responses to increasing atmospheric CO<sub>2</sub> concentrations and climate changes<sup>[4]</sup>. So far, most models generally consider the temperature sensitivity as globally invariant and use  $Q_{10}=2.0$  to simulate soil respiration. If the spatially heterogeneity in  $Q_{10}$  is considered, the direction and magnitude of the terrestrial car-

bon cycle feedbacks to climate warming could be significantly changed<sup>[5]</sup>.

Experimental studies of  $Q_{10}$  have long and extensively been conducted in many ecosystems<sup>[6]</sup>. Experimental results demonstrated that  $Q_{10}$  values varied with soil temperature<sup>[7]</sup>, quantity and quality of soil organic matter<sup>[8]</sup>, soil moisture<sup>[9]</sup> and land cover type<sup>[10]</sup>. The  $Q_{10}$  values derived from measured soil respiration and temperature usually decline with temperature because substrate availability decreases as temperature increases. As

Received March 27, 2008; accepted December 09, 2008

doi: 10.1007/s11427-009-0125-1

†Corresponding author (email: tzhou@bnu.edu.cn)

Supported by the National Natural Science Foundation of China (Grant Nos. 40671173, 40425008, 30590384 and 40401028); the Free Research Foundation of State Key Laboratory of Earth Surface Processes and Resource Ecology (Grant No. 070105)

described by the Michaelis-Menten kinetics equation, the low substrate availability generally results in a low  $Q_{10}$  value<sup>[3]</sup>. Soil water content influences temperature sensitivity because diffusivity of soluble substrates is low at low water content and diffusivity of oxygen is low at high water content. Low diffusivity of either soluble substrates at low water content or oxygen at high water content limits soil microbial respiration<sup>[3]</sup>. All the environmental and biological factors such as soil temperature, moisture, and soil organic matter are spatially heterogeneous. Accordingly, estimated  $Q_{10}$  from measured soil respiration likely varies spatially at different geographic locations<sup>[11]</sup>.

In the past,  $Q_{10}$  values have been seldom estimated using process-based modeling but mostly by regression analysis of measured soil respiration rates against temperature<sup>[12]</sup>. As empirical regression models do not contain equations to describe underlying physiological processes, the estimated  $Q_{10}$  values may not reflect temperature sensitivity of the physiological processes. High values of  $Q_{10}$  estimations, such as those significantly higher than 2.5, may be caused by confounding factors, e.g., substrate supply<sup>[3]</sup>. In addition, reliability of the estimated  $Q_{10}$  values also depends on the precision of instruments used in soil respiration measurement. The static-chamber, for example, may underestimate soil respiration<sup>[12]</sup>.

Inverse modeling can be potentially a useful method to estimate temperature sensitivity of soil respiration<sup>[13]</sup>. This method combines data from observations and experiments with a process-based biogeochemical model. For example, Ise and Moorcroft<sup>[14]</sup> applied an inverse modeling method integrating a Century-based mechanistic decomposition model with observed soil organic carbon content to estimate the optimal  $Q_{10}$  of soil respiration at the global scale. Based on the TECO-R model (Terrestrial Ecosystem Regional model) and remote sensing data, inverse modeling was also used by Zhou and Luo<sup>[15]</sup> to estimate spatial distribution of carbon residence time.

In this study, we use an inverse modeling approach to retrieve the spatial distribution of  $Q_{10}$  in China at 8 km spatial resolution. A process-based ecosystem model (CASA model) is used in combination with the measured soil organic carbon (SOC). The estimated  $Q_{10}$  values from inverse analysis are compared with those derived from observations. We also analyze the statistical

dependencies of  $Q_{10}$  values on environmental factors at the regional scale. Finally, we use a soil respiration model<sup>[12]</sup> with spatially invariant vs. heterogeneous  $Q_{10}$  values to evaluate their impacts on modeled soil respiration in response to climate warming.

## 1 Methods and materials

### 1.1 The model, data, and inverse analysis algorithm

Storage and variation of soil organic carbon (SOC) depend on soil carbon input originated from ecosystem production and soil carbon output via soil respiration. Soil respiration itself is related to  $Q_{10}$  values, climatic factors, chemical and physical properties of SOC, and soil texture<sup>[1]</sup>. Therefore, the storage of SOC at a specific site is controlled by  $Q_{10}$ , climatic factors, soil properties, and ecosystem production. During the long-term process of soil development, organic carbon gradually accumulates in soil and evolves towards a steady state without much net change in SOC under a quasi-equilibrium climate regime<sup>[16]</sup>.

In this study, we integrate a biogeochemical model Carnegie-Ames-Stanford Approach (CASA)<sup>[17,18]</sup> with measured SOC, the corresponding environmental factors at each spatial grid to estimate the optimal  $Q_{10}$  values in China. Basically, the NPP-submodel of CASA is used to constrain carbon input and the soil carbon transfer submodel together with the estimated  $Q_{10}$  is used to constrain carbon efflux, assuming that carbon influx and efflux of soil carbon pools are in equilibrium. Therefore, given these observed SOC and environmental factors, the optimal  $Q_{10}$  value at a specific site is estimated by minimizing the deviations of the observed and modeled SOC.

The data sets of measured SOC used in this study are from the Second National Soil Survey of China, which recorded 2473 typical soil profiles<sup>[19]</sup>. The NDVI data set for the period 1982 to 1999 is the standard 8-km bi-monthly continental product of Global Inventory Monitoring and Modeling Studies (GIMMS) group, available at website <http://glcf.umiacs.umd.edu/>. The meteorological data required as input for the CASA include monthly mean temperature, precipitation, and solar radiation. These data sets are provided by China Meteorological Data Sharing Service System at website <http://cdc.cma.gov.cn/>. The data sets of soil and vegetation types come from the 1 : 4000000 maps that are

compiled by the institute of Geographic Sciences and Natural Resources Research, CAS. All of those global data sets are re-sampled to the same geographic projection and spatial resolution.

At each spatial grid  $x$ , we search for the optimal value of  $Q_{10}$  in the domain  $Q \in [Q_{\min}, Q_{\max}]$  such that

$$|S_{m,x}(Q_{10}^0(Q)) - S_{0,x}| \leq |S_{m,x}(Q'_{10}) - S_{0,x}|, \forall Q'_{10} \in Q \quad (1)$$

where  $S_{0,x}$  is measured SOC in a spatial grid  $x$  at the top soil layer (0–30 cm),  $S_{m,x}(Q_{10}^0(Q))$  is the modeled SOC at the top soil layer with the optimal  $Q_{10}$  value ( $Q_{10}^0$ ) within the permissible domain  $Q$ .  $S_{m,x}(Q'_{10})$  is modeled SOC with an arbitrary  $Q_{10}$  value ( $Q'_{10}$ ) that locates in the domain  $Q$ . After the optimal  $Q_{10}$  values for all grids are estimated, the modeled mean SOC in China has the minimal deviation with the mean observations:

$$J(Q) = \frac{\sum_x |S_{m,x}(Q_{10}^0(x)) - S_{0,x}| \times a(x)}{\sum_x a(x)} \quad (2)$$

where  $a(x)$  is grid area of  $x$ , and  $J$  is the mean deviation between the modeled and observed SOC, which depends on the optimal  $Q_{10}$  value of each grid.

The permissible domain is defined by its low and upper limits ( $Q_{\min}$  and  $Q_{\max}$ , respectively). It is relatively easy to assign  $Q_{\min}$  to be 1, which means that soil respiration does not change with temperature. It is, however, somewhat difficult to define a reasonable  $Q_{\max}$ . Estimated  $Q_{10}$  values from soil respiration measurements change greatly and sometimes are very high (>10). Davidson et al.<sup>[3]</sup> argued that the estimated  $Q_{10}$  values significantly above 2.5 are unreasonable and they are probably attributed to some confounding processes and/or factors, such as substrate supply. In this study, we did not set  $Q_{\max}$  value in advance, instead, we constrain it using a prior knowledge, i.e., the optimal  $Q_{\max}$  should make the estimated mean  $Q_{10}$  value in China match with the mean value derived from soil respiration measures.

## 1.2 Verification

To examine whether or not the spatial patterns of  $Q_{10}$  values estimated from the inverse analysis algorithm are reasonable, we compiled data of  $Q_{10}$  values derived from soil respiration measurements. The ecosystems used in this verification include forests, grasslands, meadows, and croplands. We compared our estimated  $Q_{10}$  values using the inverse analysis with those derived from

measured soil respiration at different spatial locations.

## 1.3 Evaluation of $Q_{10}$ on soil respiration modeling

To evaluate the potential influences of spatially heterogeneous  $Q_{10}$  values on soil respiration in response to climate warming, we first use a soil respiration model by Raich et al.<sup>[12]</sup> to simulate the enhancement of soil respiration by assuming that temperature uniformly increases 1°C in China. The original Raich's model uses an invariant  $Q_{10}$  value ( $Q_{10}=1.72$ ) and expresses as:

$$\text{Model A: } R_s = f \times e^{(b \times T_a)} \times [P / (k + P)], \quad (3)$$

where  $R_s$  refers to the mean monthly soil respiration in g C/m<sup>2</sup>·d;  $b$  is a constant temperature sensitivity ( $b = \ln Q_{10} / 10 = 0.054$ );  $T_a$  refers to the mean monthly air temperature (°C), and  $P$  is the mean monthly precipitation (cm);  $f$  and  $k$  are constants ( $f=1.250$  and  $k=4.259$ ).

The modified model uses the estimated spatial pattern of  $Q_{10}$  value and expresses as:

$$\text{Model B: } R'_s = f \times e^{(b_x \times T_a)} \times [P / (k + P)], \quad (4)$$

where  $b_x$  is our estimated temperature sensitivity at spatial grid  $x$  ( $b_x = \ln Q_{10}(x) / 10$ );  $R'_s$  refers to the updated mean monthly soil respiration in g C/m<sup>2</sup>·d.

## 2 Results and discussion

### 2.1 Spatial pattern of estimated $Q_{10}$ values

The spatial pattern of the optimally estimated  $Q_{10}$  values at regional scale shows large spatial heterogeneity (Figure 1). Eastern China has apparently higher  $Q_{10}$  values than western China. This is probably caused by the

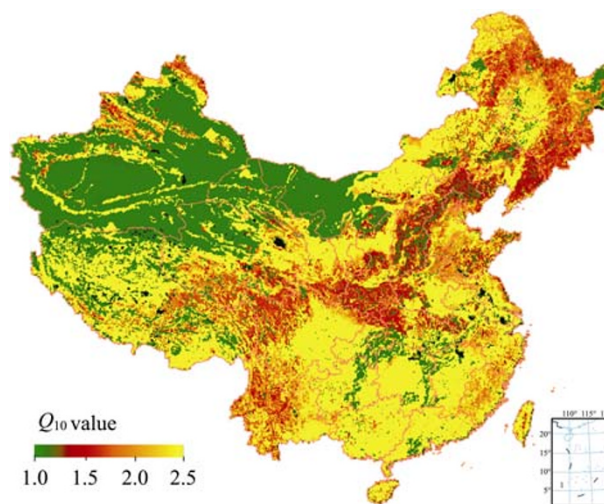


**Figure 1** Spatial distribution of temperature sensitivity of soil respiration ( $Q_{10}$  value).

typical monsoon climate in eastern China which produces warmer and moist condition and, therefore, higher productivity<sup>[20]</sup> and soil organic carbon content<sup>[21]</sup>. The good environmental condition, in turn, mitigates the environmental constraints on observed response of soil respiration to temperature and then causes higher temperature sensitivity<sup>[3]</sup>.

The mean  $Q_{10}$  values of different soil types range from 1.09 to 2.38, with the highest value in volcanic soil and the lowest value in cold brown calcic soil (Table 1). Forest soils have the highest mean  $Q_{10}$  and a relative small standard deviation ( $2.11 \pm 0.43$ ), while grassland soils have a lower mean value and a relative high spatial variation ( $2.01 \pm 0.61$ ). Cropland soils have a moderate  $Q_{10}$  value ( $2.08 \pm 0.45$ ), which is matched with their

moderate ecosystem productivity and soil moisture condition. For whole China, the mean  $Q_{10}$  value is 1.80.

The estimated optimal  $Q_{10}$  value at any specific grid is related to the range of the domain  $Q$ . When  $Q_{max}$  equals 2.5, the estimated  $Q_{10}$  values are best matched with the observation-based  $Q_{10}$  values. This is consistent with the study conducted by Davidson et al.<sup>[3]</sup>. They consider  $Q_{10}$  value significantly above 2.5 is unusual and probably caused by ignorance of some site-specific process of substrate supply.

## 2.2 Verification

The estimated  $Q_{10}$  values are well correlated with the observed  $Q_{10}$  values across wide ranges of different ecosystems (Figure 2). The observed  $Q_{10}$  values coming

**Table 1** Averaged  $Q_{10}$  values for different soil types

Soil type	$Q_{10}$ value	Soil type	$Q_{10}$ value
Latosol	1.78	Limestone soil	2.08
Latosolic red soil	2.21	Volcanic soil	2.38
Red soil	1.87	Purple soil	1.88
Yellow soil	2.10	Skeletal soil	1.29
Yellow-brown soil	1.65	Lithosol	1.26
Yellow-cinnamon soil	1.77	Meadow soil	1.85
Brown soil	1.54	Fluvo-aquic soil	1.70
Dark brown soil	1.61	Sajiang black soil	2.21
Baijiang soil	1.37	Shrub meadow soil	1.85
Brown coniferous forest soil	2.04	Mountain meadow soil	2.23
Dry red soil	1.47	Bog soil	1.85
Cinnamon soil	1.63	Solonchak	1.72
Gray cinnamon soil	2.11	Coastal solonchak	1.77
Black soil	1.86	Acid sulphate soil	1.45
Gray forest soil	1.57	Frigid plateau solonchak	2.01
Chernozem	2.05	Solonetz	1.68
Chestnut soil	2.12	Paddy soil	2.17
Castano cinnamon soil	1.68	Irrigated silting soil	1.78
Heilu soil	2.23	Irrigated desert soil	1.91
Brown calcic soil	1.65	Felty soil	1.90
Sierozem	2.14	Dark felty soil	1.89
Gray desert soil	1.09	Frigid calcic soil	1.92
Gray-brown desert soil	1.13	Cold calcic soil	1.63
Brown desert soil	1.11	Cold brown calcic soil	1.03
Loessal soil	1.75	Alpine frost desert soil	1.10
Red clay	1.72	Cold desert soil	1.67
Alluvial soil	2.01	Alpine frost soil	1.36
Takyr	1.31	Others	1.27
Aeolian sandy soil	1.19		

from peer-reviewed literatures are derived from the regression between measured soil respiration and temperature (Table 2). The estimated  $Q_{10}$  values come from the spatial pattern in Figure 1 and the grids that contain the coordinates of the observed  $Q_{10}$  values are selected. The significant correlation ( $r=0.70$ ) between estimated and measured  $Q_{10}$  indicates that the inverse modeling approach used in this study is adequate.

The  $Q_{10}$  values estimated in this study have some different spatio-temporal characteristics from those derived from field observations of soil respiration. Soil organic carbon originates from ecosystem production and it accumulates slowly in soil to a near steady state<sup>[16]</sup>. Therefore, the estimated  $Q_{10}$  values from the observations of soil organic carbon are multi-year averaged

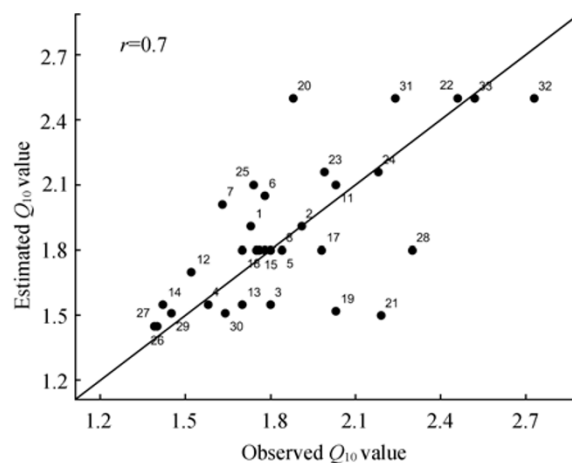


**Figure 2** Comparison between the estimated and observed  $Q_{10}$  values. Number indicates the site number listed in Table 2.

**Table 2** Comparison between observed and estimated  $Q_{10}$  values

No.	Longitude	Latitude	Ecosystem type	Observed	Estimated	Reference
1	115.05	26.73	subtropical pinus plantation	1.73	1.91	[22]
2	115.05	26.73	subtropical pinus plantation	1.91	1.91	[22]
3	128.08	42.40	temperate broad-leaved pine mixed forest	1.80	1.55	[22]
4	128.08	42.40	temperate broad-leaved pine mixed forest	1.58	1.55	[22]
5	116.82	43.51	cropland	1.84	1.80	[23]
6	116.57	43.80	cropland	1.78	2.05	[23]
7	116.31	43.91	cropland	1.63	2.01	[23]
8	116.82	43.51	grassland	1.84	1.80	[24]
9	116.69	43.63	grassland	1.75	1.80	[24]
10	116.57	43.80	grassland	1.78	1.80	[24]
11	112.55	23.17	mixed forest	2.03	2.10	[25]
12	110.75	39.60	grassland	1.52	1.70	[26]
13	116.50	39.67	Quercus Liaotungensis forest	1.70	1.55	[27]
14	116.50	39.67	Quercus Liaotungensis forest	1.42	1.55	[27]
15	120.70	42.92	degraded grassland	1.80	1.80	[28]
16	115.53	43.43	grassland	1.76	1.80	[29]
17	115.53	43.43	grassland	1.98	1.80	[29]
18	115.53	43.43	grassland	1.70	1.80	[29]
19	101.27	21.93	tropical seasonal rain forest	2.03	1.52	[30]
20	112.54	23.17	mixed forest	1.88	2.50	[31]
21	128.47	42.40	needled forest	2.19	1.50	[32]
22	123.75	44.75	meadow steppe	2.46	2.50	[33]
23	105.45	31.27	grassland	1.99	2.16	[34]
24	105.45	31.27	grassland	2.18	2.16	[34]
25	123.37	41.52	cropland	1.74	2.10	[35]
26	118.25	26.55	mid-subtropical plantation	1.40	1.45	[36]
27	118.25	26.55	mid-subtropical plantation	1.39	1.45	[36]
28	91.08	30.85	alpine steppe-meadow	2.30	1.80	[37]
29	133.52	47.58	cropland	1.45	1.51	[38]
30	133.52	47.58	cropland	1.64	1.51	[38]
31	112.53	23.18	broad-leaved evergreen forest	2.24	2.50	[39]
32	112.53	23.18	broad-leaved evergreen forest	2.73	2.50	[39]
33	112.53	23.18	mixed forest	2.52	2.50	[40]

temperature sensitivity, which is somewhat different from those derived from the momentary soil respiration measurements. So the spatial pattern of  $Q_{10}$  values in this study is more suitable for projecting long-term climate-carbon cycle feedback at large spatial scales.

### 2.3 Statistical dependency of $Q_{10}$ on environmental factors

We further calculate the relationship of estimated  $Q_{10}$  value with environmental factors.  $Q_{10}$  values are significantly correlated with the environmental factors, especially soil organic carbon content and precipitation (Figures 3 and 4). The correlation coefficient between  $Q_{10}$  and  $\ln(\text{SOC})$  is 0.69. Similar positive correlations of  $Q_{10}$  with soil organic content were reported by Taylor et al.<sup>[41]</sup> and Zhang et al.<sup>[38]</sup>. There is also a significant positive correlations between  $Q_{10}$  and precipitation ( $r=0.45$ ).

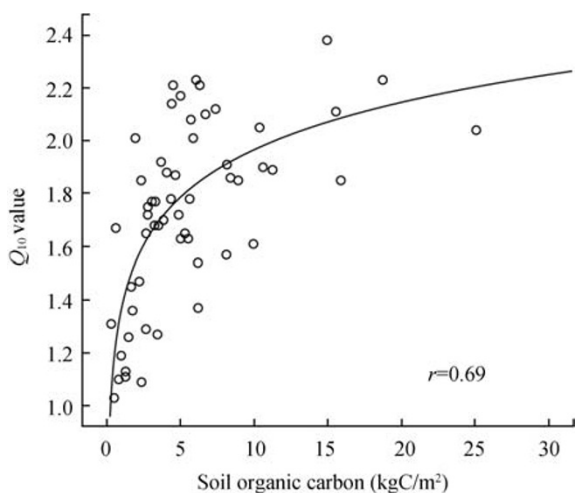


**Figure 3** Relationship between  $Q_{10}$  value and organic carbon density in top layer (0–30 cm).

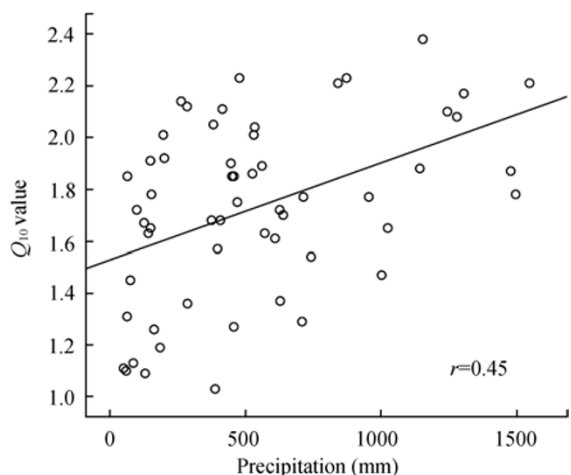


**Figure 4** Relationship between  $Q_{10}$  value and precipitation

Soil moisture is usually positively correlated with the  $Q_{10}$ <sup>[42]</sup>, as precipitation and soil moisture will affect the diffusion of soluble substrates<sup>[3]</sup>.

### 2.4 Feedback of soil respiration on temperature

The enhancement of soil respiration by 1°C temperature increase displays quite different patterns using constant  $Q_{10}$  model A (Eq. 3) and heterogeneous  $Q_{10}$  model B (Eq. 4) (Figure 5). While the general trends and spatial patterns of soil respiration enhancement are comparable between these two models, model B reveals more spatially-detailed information. The differences not only reflect spatial distribution of climatic factors but also  $Q_{10}$ 's distribution that is related to spatial patterns of SOC content, vegetation type, and ecosystem productivity.

Model A predicts 23.04 gC/m<sup>2</sup>·yr more carbon release,

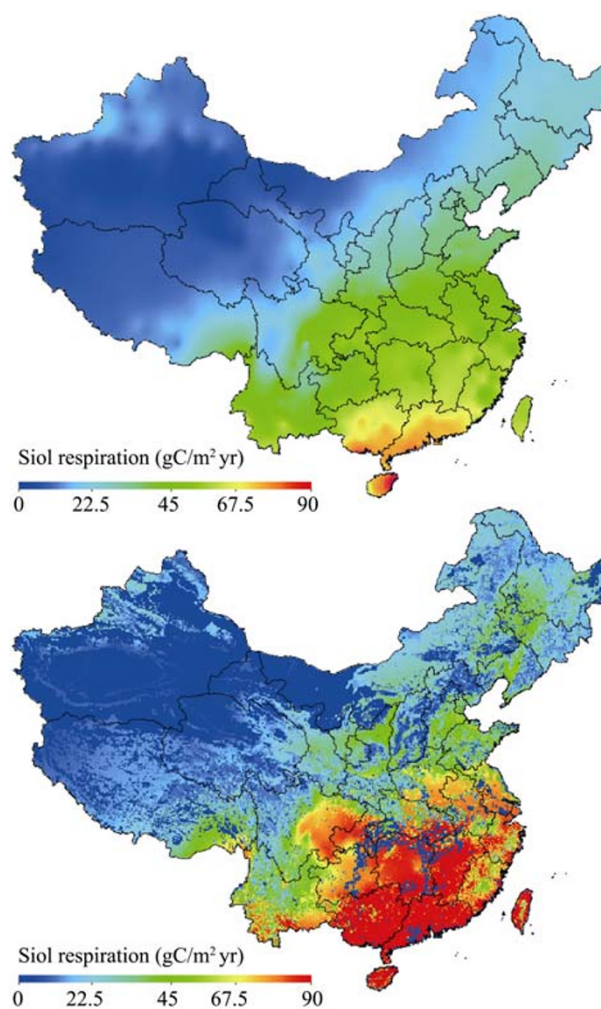


**Figure 5** Simulated enhancement of soil respiration as temperature is uniformly increasing 1°C (Top, Model A using constant  $Q_{10}$  value; Bottom, Model B using estimated spatial pattern of  $Q_{10}$  values).

while model B predicts 34.84 gC/m<sup>2</sup>·yr. It seems that if the spatial heterogeneity is ignored, the constant  $Q_{10}$  model A will underestimate temperature feedback by 33.8%. This magnitude is close to the global mean of 25% reported by Jones et al.<sup>[5]</sup>, who applied El Niño-Southern Oscillation (ENSO) and volcanic eruptions information to estimate the uncertainties of  $Q_{10}$  value and related soil respiration feedback.

### 3 Conclusions

Temperature sensitivity of soil respiration (i.e.,  $Q_{10}$  value) and its spatial distribution pattern are critical for accurate projections of future climate change and atmospheric CO<sub>2</sub> concentration. We used the inverse modeling approach to retrieve the spatial pattern of  $Q_{10}$  values by integrating the observed soil organic carbon content with a biogeochemical model. The estimates of spatially heterogeneous  $Q_{10}$  values match well with

those derived from observations of soil respirations at different sites. Our regression analysis indicates that  $Q_{10}$  values are linearly correlated ( $r=0.45$ ) with precipitation and logarithmically correlated ( $r=0.69$ ) with soil organic carbon content of top layer (0–30 cm). Incorporating the spatial heterogeneity of  $Q_{10}$  values into a soil respiration model under global warming circumstance provides a better estimation of spatial pattern of soil respiration enhancement.

*The authors thank three anonymous reviewers for their constructive suggestions. The authors are grateful to Professor Chris Field for providing the source codes of CASA model, Dr. WANG ShaoQiang for providing the observation data of soil organic carbon, China Meteorological Data Sharing Service System for providing the climatic data, Global Inventory Monitoring and Modeling Studies (GIMMS) group for providing the NDVI data sets.*

- 1 Schimel D S, Braswell B H, Holland E A, et al. Climatic, edaphic, and biotic controls over storage and turnover of carbon in soils. *Glob Biogeochem Cycle*, 1994, 8: 279–293
- 2 Luo Y. Terrestrial carbon cycle feedback to climate warming. *Annu Rev Ecol Evol Syst*, 2007, 38: 683–712
- 3 Davidson E A, Janssens I A, Luo Y. On the variability of respiration in terrestrial ecosystems: moving beyond  $Q_{10}$ . *Glob Change Biol*, 2006, 12: 154–164
- 4 Cao M K, Woodward F I. Dynamic responses of terrestrial ecosystem carbon cycling to global climate change. *Nature*, 1998, 393: 249–252
- 5 Jones C D, Cox P, Huntingford C. Uncertainty in climate-carbon-cycle projections associated with the sensitivity of soil respiration to temperature. *Tellus Ser B-Chem Phys Meteorol*, 2003, 55: 642–648
- 6 Luo Y, Zhou X. *Soil Respiration and the Environment*. San Diego: Academic Press, 2006. 1–320
- 7 Luo Y, Wan S, Hui D, et al. Acclimatization of soil respiration to warming in a tall grass prairie. *Nature*, 2001, 413: 622–625
- 8 Wan S Q, Luo Y Q. Substrate regulation of soil respiration in a tall-grass prairie: Results of a clipping and shading experiment. *Glob Biogeochem Cycle*, 2003, 17: 1054
- 9 Hui D, Luo Y. Evaluation of soil CO<sub>2</sub> production and transport in Duke Forest using a process-based modeling approach. *Glob Biogeochem Cycle*, 2004, 18: GB4029
- 10 Raich J W, Tufekcioglu A. Vegetation and soil respiration: Correlations and controls. *Biogeochemistry*, 2000, 48: 71–90
- 11 Xu M, Qi Y. Spatial and seasonal variations of  $Q_{10}$  determined by soil respiration measurements at a Sierra Nevada forest. *Glob Biogeochem Cycle*, 2001, 15: 687–696
- 12 Raich J W, Potter C S, Bhagawati D. Interannual variability in global soil respiration, 1980–94. *Glob Change Biol*, 2002, 8: 800–812
- 13 Raupach M R, Rayner P J, Barrett D J, et al. Model-data synthesis in terrestrial carbon observation: methods, data requirements and data uncertainty specification. *Glob Change Biol*, 2005, 11, 378–397
- 14 Ise T, Moorcroft P R. The global-scale temperature and moisture dependencies of soil organic carbon decomposition: an analysis using a mechanistic decomposition model. *Biogeochemistry*, 2006, 80: 217–231
- 15 Zhou T, Luo Y. Spatial patterns of ecosystem carbon residence time and NPP-driven carbon uptake in the conterminous United States. *Glob Biogeochem Cycle*, 2008, 22, GB3032
- 16 Cannell M G R, Thornley J H M. Ecosystem productivity is independent of some soil properties at equilibrium. *Plant Soil*, 2003, 257: 193–204
- 17 Potter C S, Randerson J T, Field C B, et al. Terrestrial ecosystem production: A process model based on global satellite and surface data. *Glob Biogeochem Cycle*, 1993, 7: 811–841
- 18 Field C B, Randerson J T, Malmstrom C M. Global net primary production: combining ecology and remote sensing. *Remote Sens Environ*, 1995, 51: 74–88
- 19 Wang S, Tian H, Liu J, et al. Pattern and change of soil organic carbon storage in China: 1960s–1980s. *Tellus Ser B-Chem Phys Meteorol*, 2003, 55: 416–427
- 20 Sun R, Zhu Q. Estimation of net primary productivity in China using remote sensing data. *J Geogr Sci*, 2001, 11: 14–23
- 21 Zhou T, Shi P, Luo J, et al. Estimation of soil organic carbon based on remote sensing and process model. *J Remote Sens (in Chinese)*, 2007, 11: 127–136
- 22 Yu G, Wen X, Li Q, et al. Seasonal patterns and environmental control of ecosystem respiration in subtropical and temperate forests in China. *Sci China Ser D-Earth Sci*, 2005, 48(S1), 93–105
- 23 Chen Q, Li L, Han X, et al. Temperature sensitivity of soil respiration in relation to soil moisture in 11 communities of typical temperature steppe in Inner Mongolia. *Acta Ecol Sin (in Chinese)*, 2004, 24:

- 24 Chen Q, Li L, Han X, et al. Responses of soil respiration to temperature in eleven communities in Xilingol grassland, inner Mongolia. *Acta Phytoecol Sin* (in Chinese), 2003, 27: 441—447
- 25 Deng Q, Liu S, Liu J, et al. Contributions of litter-fall to soil respiration and its affecting factors in southern subtropical forests of China. *Adv Earth Sci* (in Chinese), 2007, 22: 976—986
- 26 Guo T. Studies on soil respiration under different land use types in Wufendi Gou Basin of Huang Fu Chuan region. Master Degree Thesis (in Chinese). Huhehaote: Inner Mongolia University, 2006
- 27 Jiang G, Huang Y. A study on the measurement of CO<sub>2</sub> emission from the soil of the simulated *Quercus Liaotungensis* forest sampled from Beijing mountain areas. *Acta Ecol Sin* (in Chinese), 1997, 17: 477—482
- 28 Li Y, Zhao H, Zhao X, et al. Effects of soil temperature and moisture on soil respiration in different sand dune types. *Journal of Arid Land Resour Environ* (in Chinese), 2006, 20: 154—158
- 29 Liu L, Dong Y, Qi Y, et al. Study on the temperature sensitivity of soil respiration in Xilin River of Inner Mongolia, China. *China Environ Sci* (in Chinese), 2007, 27: 226—230
- 30 Sha L, Zheng Z, Tang J, et al. Soil respiration in tropical seasonal rain forest in Xishuangbanna, SW China. *Sci China Ser D-Earth Sci*, 2005, 48 (S1): 189—197
- 31 Wang C, Zhou G, Tang X, et al. Ecosystem respiration and its controlling factors in a coniferous and broadleaved mixed forest in Dinghushan, China. *Acta Ecol Sin* (in Chinese), 2007, 27: 2659—2668
- 32 Wang M, Ji L, Li Q, et al. Effects of soil temperature and moisture on soil respiration in different forest types in Changbai Mountain. *Chin J Appl Ecol* (in Chinese), 2003, 14: 1234—1238
- 33 Wang W, Guo J. The contribution of root respiration to soil CO<sub>2</sub> efflux in *Puccinellia tenuiflora* dominated community in a semi-arid meadow steppe. *Chin Sci Bull*, 2006, 51: 697—703
- 34 Wang X, Zhu B, Wang Y, et al. Soil respiration and its sensitivity to temperature under different land use conditions. *Acta Ecol Sin* (in Chinese), 2007, 27: 1960—1968
- 35 Wang C, Wang S, Gu J, et al. Soil Respiration in Maize Fields in the Lower Reaches of Liaohe Plain. *Journal of Agro-Environ Sci* (in Chinese), 2006, 25: 1240—1244
- 36 Wei H, Ma X. Dynamics of soil respiration in three major plantations in mid-subtropical zone. *J Fujian Agric For Univ* (in Chinese), 2006, 35: 272—277
- 37 Zhang D, Shi P, He Y, et al. Quantification of soil heterotrophic respiration in the growth period of alpine steppe-meadow on the Tibetan Plateau. *J Nat Resour* (in Chinese), 2006, 21: 458—364
- 38 Zhang J, Song C, Yang W Y. Temperature sensitivity of soil respiration and its effecting factors in the different land use. *Acta Sci Circum* (in Chinese), 2005, 25: 1537—1542
- 39 Zhou C, Zhou G, Zhang D, et al. CO<sub>2</sub> efflux different forest soils and impact factors in Dinghushan Mountain, China. *Sci China Ser D-Earth Sci*, 2005, 48: 198—206
- 40 Zhou C, Zhou G, Wang Y, et al. Soil respiration of a coniferous and broad-leaved mixed forest in Dinghushan Mountain, Guangdong Province. *J Beijing For Univ* (in Chinese), 2005, 27: 23—27
- 41 Taylor B R, Parkinson D, Parsons W F J. Nitrogen and lignin content as predictors of litter decay rates: a microcosm test. *Ecology*, 1989, 70: 97—104
- 42 Yuste J C, Janssens I A, Carrara A, et al. Interactive effects of temperature and precipitation on soil respiration in a temperate maritime pine forest. *Tree Physiol*, 2003, 23: 1263—1270